

pubs.acs.org/jasms Article

DBDA Matrix Increases Ion Abundance of Fatty Acids and Sulfatides in MALDI-TOF and Mass Spectrometry Imaging Studies

Nigina Khamidova,[†] Melissa R. Pergande,[†] Koralege C. Pathmasiri, Rida Khan, Justin T. Mohr, and Stephanie M. Cologna*



Cite This: J. Am. Soc. Mass Spectrom. 2023, 34, 1593–1597



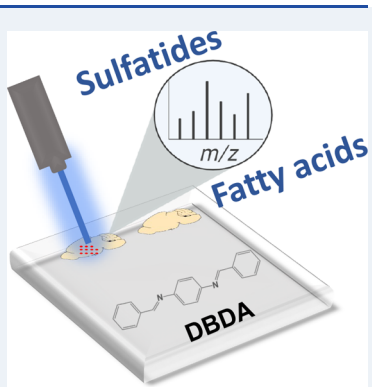
ACCESS I

III Metrics & More

Article Recommendations

s Supporting Information

ABSTRACT: MALDI-TOF MS is a powerful tool to analyze biomolecules, owing to its soft ionization nature that generally results in simple spectra of singly charged ions. Implementation of the technology in the imaging mode provides a means to spatially map analytes in situ. Recently, a new matrix, DBDA (N1,N4-dibenzylidenebenzene-1,4-diamine) was reported to facilitate the ionization of free fatty acids in negative ion mode. Building on this finding, we sought to implement DBDA for MALDI mass spectrometry imaging studies in brain tissue and successfully map oleic acid, palmitic acid, stearic acid, docosahexaenoic acid, and arachidonic acid using mouse brain sections. Moreover, we hypothesized that DBDA would provide superior ionization for sulfatides, a class of sulfolipids with multiple biological functions. Herein, we also demonstrate that DBDA is ideal for MALDI mass spectrometry imaging of fatty acids and sulfatides in brain tissue sections. Additionally, we show enhanced ionization of sulfatides using DBDA compared with three different traditionally used MALDI matrices. Together these results provide new opportunities for studies to measure sulfatides by MALDI-TOF MS.



■ INTRODUCTION

Matrix assisted laser desorption/ionization-time-of-flight mass spectrometry (MALDI-TOF MS) has enabled the rapid analysis of biomolecules from an array of sample types owing to the soft ionization nature and generation of primarily singly charged ions. With the advent of imaging strategies, MALDI mass spectrometry imaging (MSI) has enabled spatial mapping of biomolecules, drugs, and other analytes in situ. One such class of biomolecules, lipids, which are critical in cellular structure integrity, signaling, and energy storage have been analyzed broadly using MALDI MSI strategies. For example, fresh frozen bone samples have been imaged resulting in the discovery of unique signatures associated with bone marrow and soft tissues, and phospholipids have been mapped in a Drosophila model of amyotrophic lateral sclerosis brain tissue. Other examples include lipid mapping in cancer models,³ ischemic stroke,⁴ and of the human retina.⁵

Despite some common physiochemical properties of lipids, they are a class of biomolecules that are generally quite diverse. Fatty acids serve as the core components of other lipid classes; however, free fatty acids are endogenously synthesized or generated by lipolysis and have unique cellular roles. MSI has been performed on different model systems to investigate the spatial distribution of free fatty acids. For example, dynamics of isotopically labeled docosahexaenoic acid (DHA) and arachidonic acid (AA) were monitored in brain tissue following administration in mice. 6 Moreover, free fatty acids

with different acyl chain lengths and their respective double bond positions have been mapped in cancer tissues.⁷

Another family of bioactive lipids is sulfolipids, and one class includes sulfatides (SHexCer) which are sulfated glysosphingolipids. The biological functions of sulfatides is vast and in the brain, sulfatides are highly enriched in myelin. With regard to MSI, sulfatides have been mapped in brain tissues to understand oligodendrocyte development as well as in renal tissues of a model of Alport Syndrome. Thus, continued mapping of these crucial lipids is of the utmost importance in biological specimens such as brain tissue.

While MSI has been a successful strategy in measuring lipid distributions, the heterogeneous nature of lipids requires utilization of differing matrices and ionization modes for successful detection. Common MALDI matrices for lipid analysis include 1,5-diaminonaphthalene (DAN), α -cyano-4-hydroxycinnamic acid (CHCA), 2,5-dihydroxybenzoic acid (DHB), and 9-aminoacridine (9-AA). In a recent study, the compound N1,N4-dibenzylidenebenzene-1,4-diamine (DBDA, Figure 1), was shown to ionize small molecules (<500 Da) including free fatty acids without matrix interference. ¹¹ In this

Received: February 15, 2023 Revised: June 13, 2023 Accepted: June 15, 2023 Published: July 10, 2023





Figure 1. Chemical structure of DBDA.

study, we demonstrate using DBDA to acquire MALDI-MS images of free fatty acids as well as sulfatides from murine mouse brains. Finally, we compare the ion abundance of sulfatide standards with commonly used MALDI matrices versus DBDA.

MATERIALS AND METHODS

Reagents. Sulfatides standards were obtained from Avanti Polar Lipids (Alabaster, AL). LC-MS grade acetonitrile (ACN), methanol (MeOH), 9-aminoacridine (9-AA), α-cyano-4-hydroxycinnamic acid (CHCA), bradykinin 2–9, angiotensin I and II, ACTH 18–39, and ammonium formate were obtained from Sigma-Aldrich (St. Louis, MO). 1,5-Diaminonaphthalene (DAN) was obtained from TCI Chemicals (Portland, OR). Tissue-Tek O.C.T. compound was received from Sakura Finetek (Torrance, CA). N1,N4-Dibenzylidene benzene-1,4-diamine (DBDA) was synthesized as previously described, 11 and purity was determined to be greater than 95%.

Experimental Model. All experiments were performed in accordance with the University of Illinois Chicago IACUC approved protocols. Heterozygous Balb/c Npc^{nih} ($Npc1^{\pm}$) mice were obtained from Jackson Laboratories (RRID: IMSR JAX:003092) and a breeding colony were maintained in our laboratory. Genotyping was performed using polymerase chain reaction as previously described. Control ($Npc1^{+/+}$) mice at 10 weeks of age were euthanized by CO_2 asphyxiation and subsequently decapitation. Whole brain tissue from control mice was dissected and immediately frozen on dry ice to

maintain spatial integrity and stored at $-80~^{\circ}\text{C}$ until further use.

Sample Preparation. A CryoStar NX50 Cryostat (Thermo Fisher Scientific) was used to cryosection frozen, intact brain tissue at $-11\,^{\circ}$ C. Eight serial sagittal sections from wild type brains were obtained at 10 μ m thickness, thawmounted directly on a MALDI stainless steel target plate, and stored at $-80\,^{\circ}$ C until further analysis. The tissues were thawed and washed in cold 50 mM ammonium formate solution for 15 s. The tissues were then vacuum-dried at room temperature and weighed prior to matrix application.

Matrix Sublimation. A homemade sublimation apparatus was used to apply the MALDI matrix to produce an even coating of DBDA. Forty milligrams of DBDA were solubilized in 3 mL of acetone and then aspirated onto the bottom of sublimation flask. Acetone was evaporated using a N_2 stream to form an even layer of matrix on the bottom of the sublimation flask. The hot plate was set to 128 °C, and to monitor the actual temperature of the sublimation flask, a digital thermometer probe was placed in contact with the bottom of the sublimation flask. An ice slush was placed in the coldfinger, to which the MALDI plate was adhered on the underside using copper tape. Sublimation was done under 80 mTorr pressure for 12 min. Matrix was applied at a density of 0.28 mg/cm².

Mass Spectrometry Dried-Droplet Analysis. Sulfatide standard mix was dissolved in methanol. DAN, 9-AA, and CHCA were dissolved in 70% ACN/ $\rm H_2O$, and DBDA was dissolved in 80% ACN/ $\rm H_2O$ resulting in 5 mg/mL matrix concentration. A 1:1 (v/v) ratio of matrix and a solution of 0.01 nmol/ μ L sulfatide standard were mixed before spotting on the MALDI plate. MALDI-TOF/TOF mass spectrometry was performed using a Sciex 4800 MALDI-TOF/TOF mass spectrometer equipped with a 200 Hz Nd:YAG (355 nm) laser and was externally calibrated with a calibration mix in the negative reflectron mode. Six replicate measurements were

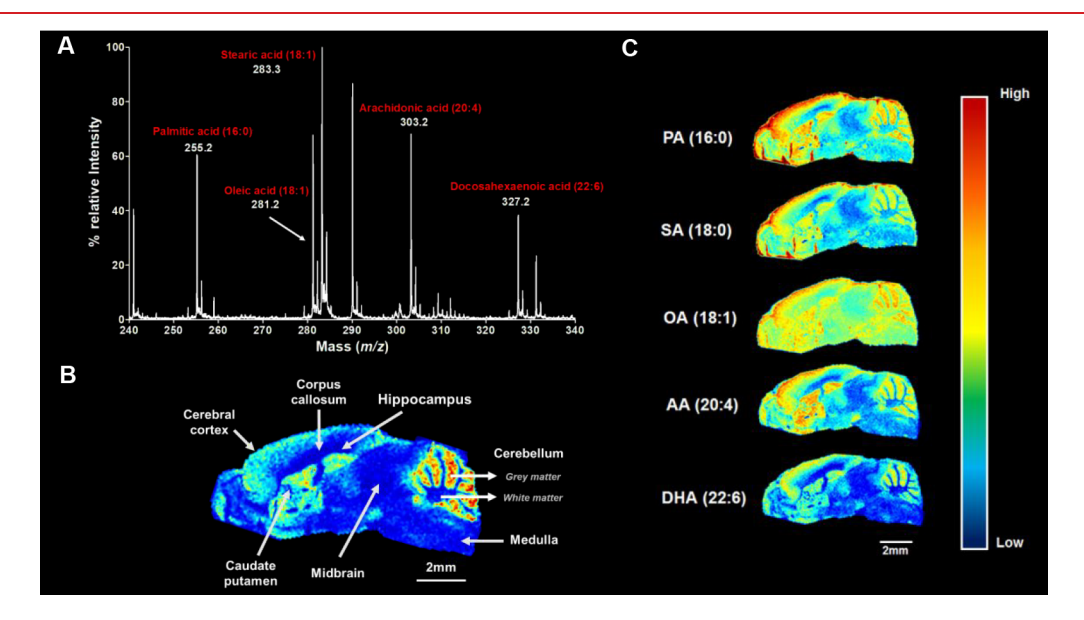


Figure 2. DBDA as a matrix for the MALDI analysis of fatty acids in murine brain tissues. N1,N4-Dibenzylidenebenzene-1,4-diamine (DBDA) was applied via sublimation at 128 °C for 12 min to 10 μ M brain tissue sections. (A) Shown is the on-tissue MALDI-TOF mass spectrum for m/z 240–340 where peaks corresponding to common brain fatty acids are annotated. (B) Ion density map of DHA (m/z 327.2) showing distinct brain regions. (C) MALDI-mass spectrometry imaging (MSI) analysis was performed on sagittal cryosections from 10-week mice. Shown are ion density maps for palmitic (PA), stearic (SA), oleic (OA), docosahexaenoic (DHA) and arachidonic acid (AA).

taken for 9 different sulfatide species. Lipid data was acquired in negative ion reflectron mode in the m/z 750–1000 range. MALDI-MS spectra were collected on dried droplet mixtures of 5 mg/mL DBDA and 0.01 nmol/ μ L ST standard mix. Seven replicates were analyzed for 21 different ST mixture dilutions using 3000 laser intensity. For laser fluence dependence studies, ST 18:1/24:1 was spotted at the same concentration (10pmol/ μ L, 5pmol on plate) and the laser intensity was varied from 2500 to 3700 arbitrary units.

MALDI Mass Spectrometry Imaging. MALDI-TOF mass spectrometry imaging was performed using a Sciex 4800 MALDI-TOF/TOF. The raster size was set to $100~\mu m$ using the 4800 Imaging Tool v3.2 (https://ms-imaging.org/wp/4000-series-imaging) and laser shots per pixel was set to 50. Data was acquired in negative ion reflectron mode with the mass range m/z 750–1000 for sulfatides and m/z 200–500 for free fatty acids. Data processing was done using MSiReader v1.0. ^{14,15} GraphPad Prism 9 was used for the statistical analysis.

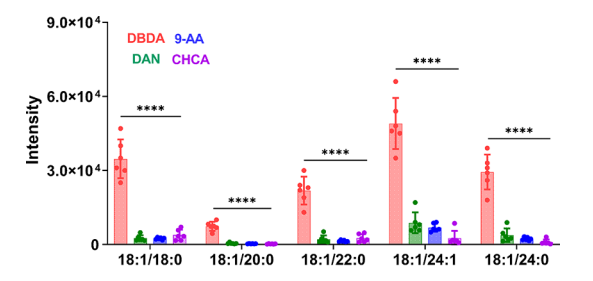
RESULTS AND DISCUSSION

Imaging lipids to visualize their spatial distribution is not widely feasible using antibody-based strategies, and mass spectrometry imaging has been a powerful tool to enable such endeavors. A challenge with lipid analysis is the need for optimized matrix conditions for different classes of lipids. As previously reported, the highly stable, DBDA matrix is an excellent choice to ionize free fatty acids in a dried-drop experiment. In the current study, we aimed to further investigate the utilization of DBDA as a matrix for lipid MSI and to explore the possibility of enhanced ion abundance of another lipid class, namely, sulfatides. The experimental workflow is depicted in Figure S1.

Spatial Distribution of Free Fatty Acids Using DBDA **as a Matrix.** We first sought to determine the appropriateness of carrying out MALDI-MSI using DBDA as the matrix for free fatty acid mapping in whole brain tissue. Using sagittal murine brain sections, we demonstrate strong signals for free fatty acids (Figure 2A). Notably, we observe clear isotopic distributions of known fatty acid masses, which are labeled in the order of palmitic acid (16:0) m/z 255.2, oleic acid (18:1) m/z 281.2, stearic acid (18:1) m/z 283.3, arachidonic acid (20:4) m/z 303.2, and docosahexaenoic acid (22:6) m/z327.2. All observed ions are $[M - H]^-$. A representative image with labeled brain features is provided in Figure 2B. Next, we generated the MALDI image for free fatty acids in 10-week-old mice (Figure 2C). We observe that most free fatty acids are localized in the gray matter of the brain. The highest ion signal for all five fatty acids arises from the cerebral cortex and the gray matter of the cerebellum. Palmitic acid (16:0) and stearic acid (18:0) exhibit high ion intensity in the cerebral cortex as well as in the outer regions of the cerebral cortex. Oleic acid (18:1) (OA (18:1)) is in higher abundance in the white matter than the other common fatty acids. A strong signal for docosahexaenoic acid (DHA) is observed to be solely localized on the gray matter of the brain. Based on these data, we can conclude that DBDA can be used to acquire the spatial distribution of free fatty acids directly from the tissue with high reliability.

DBDA Enhances Ionization of Sulfatides Compared to Other Matrices. Numerous studies using differing MALDI matrices to ionize biomolecules have been conducted. As previously reported, DAN facilitates both negative and positive

ion production and has been successfully implemented for imaging. ¹⁶ Other matrices that are useful for lipid imaging but are challenging to sublime include CHCA and 9-amino-acridine. Despite these challenges, considering the proper MALDI matrix is important to generate strong signals for the ions of interest. Given our encourging result for imaging fatty acids with DBDA, we sought to determine if ion abundance was increased compared with other standard MALDI-MS matrices for another lipid class, sulfatides. Using the dried droplet method, a standard mixture of nine of the common sulfatides was analyzed (Figure 3). The sulfatide mixture



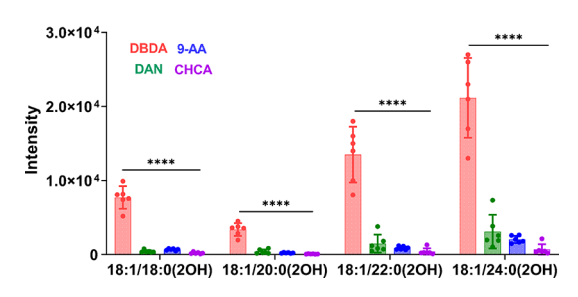


Figure 3. Comparison of different MALDI matrices for the analysis of sulfatides. Standards for both (A) nonhydroxylated and (B) 2-hydroxy sulfatides were analyzed by MALDI-MS using different matrices. For all standards, the use of the DBDA matrix resulted in a significant (one-way ANOVA, p < 0.0001 (****)) increased intensity compared to other matrices.

contained SHexCer (18:1/22:0), SHexCer (18:1/20:0)-(2OH), SHexCer (18:1/20:0), SHexCer (18:1/18:0)(2OH), SHexCer (18:1/18:0), SHexCer (18:1/24:1), SHexCer (18:1/ 24:0), SHexCer (18:1/24:0)(2OH), and SHexCer (18:1/ 22:0)(2OH). Examples of MS/MS spectra from this mixture for four lipids is provided in Figure S2. The four common matrices used in negative ion MALDI analysis that we compared were: DBDA, CHCA, 9-AA, and DAN. The same solution concentration was used for all analyses. Figure 3A displays a comparison of these matrices for four nonhydroxylated sulfatides. We observe that the nonhydroxylated sulfatides that were analyzed with DBDA matrix exhibit higher ion abundance than other three matrices with high significance, p < 0.0001 (****). The same results are seen in hydroxylated sulfatides with 18, 20, 22, and 24 acyl chains (Figure 3B). To further validate our observations that DBDA generated higher abundances compared to other matrices, we next carried out a dried droplet experiment using the same concentration of sulfatide standard with the four matrices with varying laser fluence (Figure 4). In all cases, the signals observed with DBDA as the matrix is greater than the other three matrices being evaluated indicating that even at optimized laser fluence, DBDA is superior. With these data, we conclude that DBDA

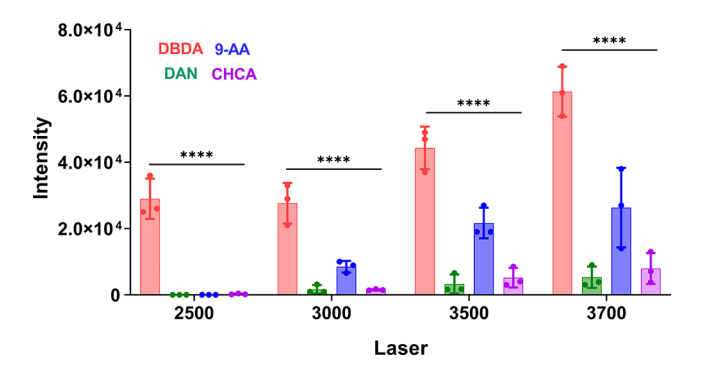


Figure 4. Comparison of different MALDI matrices and laser intensities for the analysis of sulfatides. Sulfatide standard ST (18:1/24:1) was mixed with each MALDI matrix and analyzed in triplicate for each laser intensity. The use of the DBDA matrix resulted in a significant (one-way ANOVA, p < 0.0001 (****)) increased intensity compared to other matrices at the different laser intensities tested.

enhances ionization of sulfatides when compared to DAN, 9-AA, and CHCA.

Acquiring Spatial Distributions of Sulfatides Using DBDA Matrix. We next evaluated the use of DBDA for MALDI- MSI of sulfatides. First, we investigated the on-tissue mass spectrum by acquiring data from m/z 800–910 (Figure 5A). Strong signals corresponding to the accurate mass of sulfatide lipids are observed again as $[M-H]^-$ species. We observed nine different sulfatide species with differing abundance. The most abundant sulfatide detected in mice brain tissue was SHexCer(d18:1/24:1) with m/z 888.5 $[M-H]^-$ ion. The least abundant sulfatide detected in mice brains in SHexCer (d18:1/20:0) with m/z 834.5 $[M-H]^-$ ion. Other sulfatides that were observed include SHexCer (d18:1/18:0) with m/z 806.5, SHexCer (d18:1/18:0(20H)) with m/z 822.5, SHexCer (d18:1/20:0) with m/z 850.5, SHexCer

(d18:1/22:0) with m/z 862.5, SHexCer (d18:1/22:0(2OH)) with m/z 878.5, SHexCer (d18:1/24:1(2OH)) with m/z 904.5, and SHexCer (d18:1/24:0(2OH)) with m/z 906.5. The mass spectrum indicates the capability of DBDA to ionize sulfatides, thus warranting exploration of imaging strategies. Next, we performed tissue MS/MS for these precursor ions to confirm the molecular structure and identity. On tissue MS/MS of m/z 878.5 (Figure 5B) confirmed the assignment. Key fragment ions observed include HSO₄ $^-$ (m/z 97.1), sulfated sugar group (SHex, m/z 241.1), and 22:0-OH fatty acyl chain (m/z 568.4). Figure 5C is a representative image for the spatial distribution of the hydroxylated sulfatide SHexCer d18:1/22:0 (2OH). These mass spectra and mass spectrometry images of sulfatides indicate that DBDA can be used as a matrix in MALDI-MSI to obtain a spatial distribution of sulfatides.

pubs.acs.org/jasms

CONCLUSIONS

In the current study, we sought to utilize DBDA as a negative ion MALDI matrix to image free fatty acids in brain tissues. We also compared the ion abundances of sulfatide standards using DBDA versus other commonly used MALDI matrices and found that the most abundant signal for these standards is observed when DBDA is used. Moreover, we explore the possibility of performing MSI using DBDA for the anionic sulfated lipids, sulfatides. Our data confirm the feasibility of each. This data support the notion that DBDA is an excellent MALDI matrix for both free fatty acids and sulfatides using both standard dried droplet methodologies as well as MALDI-MSI via sublimation.

ASSOCIATED CONTENT

Supporting Information

The Supporting Information is available free of charge at https://pubs.acs.org/doi/10.1021/jasms.3c00061.

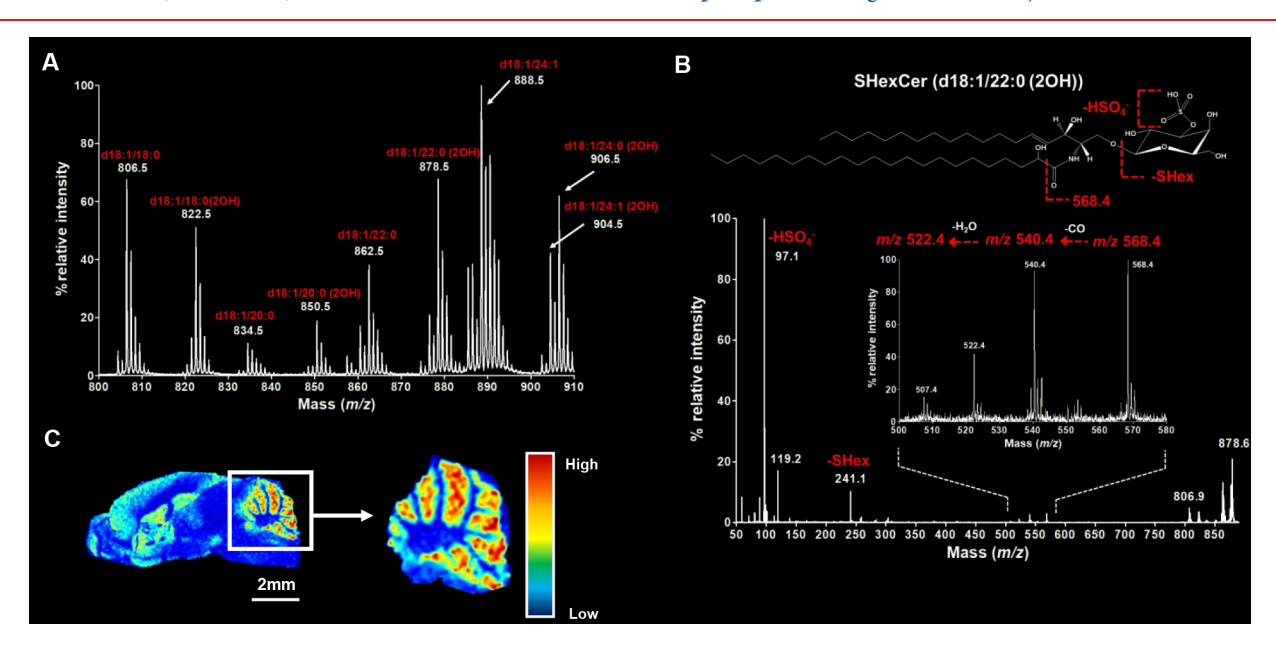


Figure 5. DBDA as a matrix for MALDI analysis of sulfatides in murine brain tissues. (A) N1, N4-dibenzylidenebenzene-1,4-diamine (DBDA) was applied via sublimation. Shown is the on-tissue MALDI average mass spectrum for m/z 800–910. Putative mass assignments for multiple sulfatides are annotated. (B) On-tissue tandem MALDI-MS/MS mass spectrum for m/z 878.5, where peaks corresponding to fragments are annotated. Here, we observed the loss of the HSO₄-(m/z 97.1), the sulfated sugar group (SHex, m/z 241.1) and 22:0-OH fatty acyl chain (m/z 568.4). (C) MALDI-mass spectrometry imaging (MSI) analysis was performed on sagittal cryosections from 10-week mice. Shown is the ion density map for SHexCer d18:1/22:0 (2OH).

Experimental workflow and tandem MS spectra of lipids (PDF)

AUTHOR INFORMATION

Corresponding Author

Stephanie M. Cologna — Department of Chemistry and Laboratory of Integrative Neuroscience, University of Illinois Chicago, Chicago, Illinois 60607, United States;
orcid.org/0000-0002-3541-3361; Email: cologna@

Authors

uic.edu

Nigina Khamidova – Department of Chemistry, University of Illinois Chicago, Chicago, Illinois 60607, United States

Melissa R. Pergande – Department of Chemistry, University of Illinois Chicago, Chicago, Illinois 60607, United States

Koralege C. Pathmasiri — Department of Chemistry, University of Illinois Chicago, Chicago, Illinois 60607, United States

Rida Khan – Department of Chemistry, University of Illinois Chicago, Chicago, Illinois 60607, United States

Justin T. Mohr — Department of Chemistry, University of Illinois Chicago, Chicago, Illinois 60607, United States;
ocid.org/0000-0002-7005-3322

Complete contact information is available at: https://pubs.acs.org/10.1021/jasms.3c00061

Author Contributions

[†]N.K. and M.R.P.: Equal contribution.

Notes

The authors declare no competing financial interest.

ACKNOWLEDGMENTS

This work was supported in part by the Department of Chemistry, University of Illinois Chicago. Additional funding is acknowledged from the National Institutes of Health, UIC Portal to Biomedical Research Careers (UIC PBRC) PREP (R25GM121212), NIA/NINDS R01NS114413, NINDS R01NS124784, and the National Science Foundation CAREER Award # 2143920.

REFERENCES

- (1) Good, C. J.; Neumann, E. K.; Butrico, C. E.; Cassat, J. E.; Caprioli, R. M.; Spraggins, J. M. High Spatial Resolution MALDI Imaging Mass Spectrometry of Fresh-Frozen Bone. *Anal. Chem.* **2022**, 94 (7), 3165–3172.
- (2) Jang, H. J.; Le, M. U. T.; Park, J. H.; Chung, C. G.; Shon, J. G.; Lee, G. S.; Moon, J. H.; Lee, S. B.; Choi, J. S.; Lee, T. G.; Yoon, S. Matrix-Assisted Laser Desorption/Ionization Mass Spectrometry Imaging of Phospholipid Changes in a Drosophila Model of Early Amyotrophic Lateral Sclerosis. *J. Am. Soc. Mass Spectrom.* **2021**, 32 (10), 2536–2545.
- (3) Sah, S.; Ma, X.; Botros, A.; Gaul, D. A.; Yun, S. R.; Park, E. Y.; Kim, O.; Moore, S. G.; Kim, J.; Fernandez, F. M. Space- and Time-Resolved Metabolomics of a High-Grade Serous Ovarian Cancer Mouse Model. *Cancers (Basel)* **2022**, *14* (9), 2262.
- (4) Andrews, W. T.; Donahue, D.; Holmes, A.; Balsara, R.; Castellino, F. J.; Hummon, A. B. In situ metabolite and lipid analysis of GluN2D(-/-) and wild-type mice after ischemic stroke using MALDI MSI. *Anal Bioanal Chem.* **2020**, 412 (24), 6275–6285.
- (5) Kotnala, A.; Anderson, D. M. G.; Patterson, N. H.; Cantrell, L. S.; Messinger, J. D.; Curcio, C. A.; Schey, K. L. Tissue fixation effects on human retinal lipid analysis by MALDI imaging and LC-MS/MS technologies. *J. Mass Spectrom* **2021**, *56* (12), e4798.

- (6) Yoshinaga, K.; Ishikawa, H.; Taira, S.; Yoshinaga-Kiriake, A.; Usami, Y.; Gotoh, N. Selective Visualization of Administrated Arachidonic and Docosahexaenoic Acids in Brain Using Combination of Simple Stable Isotope-Labeling Technique and Imaging Mass Spectrometry. *Anal. Chem.* **2020**, *92* (13), 8685–8690.
- (7) Zhang, H.; Xu, M.; Shi, X.; Liu, Y.; Li, Z.; Jagodinsky, J. C.; Ma, M.; Welham, N. V.; Morris, Z. S.; Li, L. Quantification and molecular imaging of fatty acid isomers from complex biological samples by mass spectrometry. *Chem. Sci.* **2021**, *12* (23), 8115–8122.
- (8) Takahashi, T.; Suzuki, T. Role of sulfatide in normal and pathological cells and tissues. *J. Lipid Res.* **2012**, *53* (8), 1437–50.
- (9) Hirahara, Y.; Wakabayashi, T.; Mori, T.; Koike, T.; Yao, I.; Tsuda, M.; Honke, K.; Gotoh, H.; Ono, K.; Yamada, H. Sulfatide species with various fatty acid chains in oligodendrocytes at different developmental stages determined by imaging mass spectrometry. *J. Neurochem* **2017**, *140* (3), 435–450.
- (10) Gessel, M. M.; Spraggins, J. M.; Voziyan, P. A.; Abrahamson, D. R.; Caprioli, R. M.; Hudson, B. G. Two Specific Sulfatide Species Are Dysregulated during Renal Development in a Mouse Model of Alport Syndrome. *Lipids* **2019**, *54* (6–7), 411–418.
- (11) Ling, L.; Li, Y.; Wang, S.; Guo, L.; Xiao, C.; Chen, X.; Guo, X. DBDA as a Novel Matrix for the Analyses of Small Molecules and Quantification of Fatty Acids by Negative Ion MALDI-TOF MS. J. Am. Soc. Mass Spectrom. 2018, 29 (4), 704–710.
- (12) Tobias, F.; Olson, M. T.; Cologna, S. M. Mass spectrometry imaging of lipids: untargeted consensus spectra reveal spatial distributions in Niemann-Pick disease type C1. *J. Lipid Res.* **2018**, 59 (12), 2446–2455.
- (13) Tobias, F.; Pathmasiri, K. C.; Cologna, S. M. Mass spectrometry imaging reveals ganglioside and ceramide localization patterns during cerebellar degeneration in the Npc1(-/-) mouse model. *Anal Bioanal Chem.* **2019**, *411* (22), 5659–5668.
- (14) Bokhart, M. T.; Nazari, M.; Garrard, K. P.; Muddiman, D. C. MSiReader v1.0: Evolving Open-Source Mass Spectrometry Imaging Software for Targeted and Untargeted Analyses. *J. Am. Soc. Mass Spectrom.* **2018**, 29 (1), 8–16.
- (15) Robichaud, G.; Garrard, K. P.; Barry, J. A.; Muddiman, D. C. MSiReader: an open-source interface to view and analyze high resolving power MS imaging files on Matlab platform. *J. Am. Soc. Mass Spectrom.* **2013**, 24 (5), 718–21.
- (16) Thomas, A.; Charbonneau, J. L.; Fournaise, E.; Chaurand, P. Sublimation of new matrix candidates for high spatial resolution imaging mass spectrometry of lipids: enhanced information in both positive and negative polarities after 1,5-diaminonapthalene deposition. *Anal. Chem.* **2012**, *84* (4), 2048–54.